Journal of Solid State Electrochemistry (2024) 28:1963–1970
https://doi.org/10.1007/s10008-024-05826-5

SHORT COMMUNICATION

Comparative analysis of the structure and electrical properties of single crystal and ceramic $(ZrO_2)_{0.90}(Sc_2O_3)_{0.09}(Yb_2O_3)_{0.01}$ solid electrolyte

D. A. Agarkov[1,6] · E. A. Agarkova[1] · M. A. Borik[2] · E. M. Buzaeva[3] · G. M. Korableva[1] · A. V. Kulebyakin[2] · I. E. Kuritsyna[1] · V. M. Kyashkin[3] · E. E. Lomonova[2] · F. O. Milovich[4,5] · V. A. Myzina[2] · P. A. Ryabochkina[3] · N. Yu. Tabachkova[2,4] · M. K. Tapero[2,4]

Received: 30 November 2023 / Revised: 26 January 2024 / Accepted: 27 January 2024 / Published online: 7 February 2024

Abstract

Ceramics with the composition of $(ZrO_2)_{0.90}(Sc_2O_3)_{0.09}(Yb_2O_3)_{0.01}$ was obtained by tape casting onto a moving substrate using the original powder obtained by grinding single crystals. The phase composition, crystalline, and local structure of ceramics and single crystals were studied using X-ray diffractometry, Raman, and optical spectroscopy. The electrical conductivity of the samples was measured using impedance spectroscopy methods in the temperature range of 350–900 °C. It has been shown that the phase composition, crystalline and local structure, as well as the crystal lattice parameter of ceramics do not undergo changes compared to single crystals. The technological process used for ceramics manufacture did not lead to contamination of the material with foreign impurities. The electrical conductivity of ceramic samples was less than the electrical conductivity of a single crystal over the entire temperature range. Thus, the values of electrical conductivity of ceramics and single crystals at a temperature of 1173 °K were equal to 0.176 and 0.235 S/cm, respectively. The observed differences in electrical conductivity are likely due to the presence of pores and grain boundaries in the ceramic samples.

Keywords Solid electrolytes · Zirconium dioxide · Single crystals · Phase composition · Structure · Ionic conductivity

Introduction

Currently, ceramic materials based on zirconium dioxide have oxygen ion conductivity at elevated temperatures and they are used as solid electrolytes [1–10]. Modern development of ceramic technology makes it possible to produce products of complex shapes and high density and ensures scaling of their sizes. A wide range of modern manufacturing techniques makes it possible to organize industrial production at existing enterprises. The technology for the production of ceramic solid electrolytes for electrochemical devices should provide the ability to obtain mechanically strong and dense membranes with small thicknesses and large areas, possessing the required transport characteristics with a high degree of stability at operating temperatures. The electrical characteristics and stability of ceramics under operating conditions are influenced by many factors related to the characteristics of the microstructure, such as grain sizes, heterogeneity in the distribution of components along the grain boundaries and in their volume, impurities, and pores at the grain boundaries. The characteristics of the

✉ D. A. Agarkov
agarkov@issp.ac.ru

1 Osipyan Institute of Solid State Physics RAS, Academician Osipyan Street, 2, 142432 Chernogolovka, Moscow District, Russia

2 Prokhorov General Physics Institute of Russian Academy of Sciences, Vavilova Street, 38, 119991 Moscow, Russia

3 Institute of High Technologies and New Materials, National Research Ogarev Mordovia State University, Bolshevistskaya Street, 68, 430005 Saransk, Russia

4 Department of Materials Science of Semiconductors and Dielectrics, National University of Science and Technology "MISIS", Leninskiy Prospekt, 4, 119049 Moscow, Russia

5 Department of Materials Science, Moscow Polytechnic University, Bolshaya Semyonovskaya Street, 38, 107023 Moscow, Russia

6 Moscow Institute of Physics and Technology, Institutsky Lane, 9, 141700 Dolgoprudny, Moscow Region, Russia

structure and transport properties, in turn, depend on the method of synthesis and specific temperature–time regimes for obtaining these materials [11–21].

One of the methods for the synthesis of solid solutions based on zirconium dioxide is the method of directional crystallization of the melt in a cold crucible [22]. These materials do not contain grain boundaries, and their electrical conductivity depends only on the initial composition and crystallization conditions, including the growth and cooling rates of the crystal ingot. Fast and complete synthesis in a melt from the starting oxides does not require intermediate steps, which may lead to contamination of the starting materials and, in addition, further purification from external impurities occurs during the crystallization process. This method was used to obtain crystals of ZrO_2-based solid solutions stabilized by Sc_2O3 and co-doped with oxides of rare earth elements [23–28]. However, the practical application of single-crystalline materials is limited by the requirements for size and shape, since additional costs are required for their mechanical processing.

The structure, physical, and transport properties of ceramic solid electrolytes based on Sc_2O_3-stabilized ZrO_2 и co-doped with oxides of rare earth elements are being actively studied [8, 10–17, 19].

One of the effective co-doping oxides that stabilize the highly conductive cubic phase in the ZrO_2–Sc_2O_3 binary system is Yb_2O_3 [29–31]. It has been shown that the electrical conductivity at high temperatures of these solid solutions decreases with increasing Yb_2O_3 concentration. Single-phase cubic ceramic samples of the composition $(ZrO_2)_{0.91}(Sc_2O_3)_{0.08}(Yb_2O_3)_{0.01}$, obtained by solid-phase synthesis, had the maximum conductivity (0.30 S/cm at 1273 °K) [31]. These materials also have high phase stability to high-temperature exposures and high long-term stability of electrical conductivity [29]. High stability of structural and transport characteristics during long-term exposure at a temperature of 850 °C was also observed in $(ZrO_2)_{0.90}(Sc_2O_3)_{0.09}(Yb_2O_3)_{0.01}$ single crystals [28].

The purpose of this work was to obtain ceramic solid electrolyte with the composition $(ZrO_2)_{0.90}(Sc_2O_3)_{0.09}(Yb_2O_3)_{0.01}$, using powder prepared from crushed crystals as a starting material, as well as to conduct a comparative analysis of the structure and electrical properties of single crystal and ceramic samples of this solid electrolytes.

Materials and experimental techniques

Single crystals $(ZrO_2)_{0.90}(Sc_2O_3)_{0.09}(Yb_2O_3)_{0.01}$ were grown using the method of directional crystallization of the melt in a cold crucible [22]. The starting materials used were zirconium, scandium, and ytterbium oxide powders with a purity of at least 99.99%. Small concentrations of Eu_2O_3 (no more than 0.1 mol%) were additionally introduced into the composition of some crystals, and Eu_2O_3 was used as a spectroscopic probe for spectral and luminescence studies. A part of the crystals was used to make initial powders for ceramic samples.

$(ZrO_2)_{0.90}(Sc_2O_3)_{0.09}(Yb_2O_3)_{0.01}$ single crystals were pre-ground in a Fritsch Pulverisette 6 classic line planetary mill (Germany). Grinding was carried out in ethanol using a 10-mm grinding media made of partially stabilized zirconium dioxide. Grinding mode, 400 rpm; 60 min. After grinding, the powder was dried in a SNOL drying box (Russia) at a temperature of 100 °C for 30–60 min. The determination of the average particle size of ceramic powders was carried out on an Analysette 22 NanoTec plus analyzer (Fritsch, Germany) using the laser diffraction method.

The casting suspension was prepared in a Thinky ARE-250 planetary mixer (Japan). Organic base consisting of solvents—methyl ethyl ketone (MEK) (Vekton, Russia) and ethanol, plasticizer—butyl benzyl phthalate (BBP) (Reakhim, Russia), binder—polyvinyl butyral (PVB) (Sigma Aldrich, Germany), and surfactant—N-tallow diamine (Shaanhi Dideg Medichem Co., Ltd., China) was manufactured separately. The content of the components in the casting suspension was (mass%) MEK, 44.6; ethanol, 29.5; PVB, 18.5; and BBP, 7.4. The surfactant content was 1% by weight of the powder.

Mixing was carried out in the following mode: 1000 rpm; the total mixing time was 30 min. After introducing the electrolyte powder into the final organic mixture, it was mixed in a mixer according to the following mode: 1000 rpm; the total mixing time was 1–2 h.

The casting of the finished suspension was carried out on a Lisa TTC-1000 line (USA) using a two-blade system. The level of the lifting of the first blade above the supporting polyethylene (PE) film was 800 μm, and the level of lifting of the second blade was 600 μm. The temperature at which casting was carried out was in the range of 22–23 °C. The cast tape was dried in the air for 4 h. Annealing was carried out in a high-temperature Nabertherm HTC 40/16 furnace (Germany) in air at the temperature of 1500 °C for 1 h using alumina cover plates.

The microstructure of ceramics was studied using a scanning electron microscope Supra 50VP equipped with an INCA Energy + microanalysis system.

The phase composition and structure were studied by X-ray diffraction and Raman spectroscopy. X-ray diffraction studies were carried out using an Empyrean diffractometer manufactured by PANalitical B.V. (CuKα radiation, $\lambda = 1.5414$ Å) with a vertical goniometer and a PIXcel 3D detector, respectively. To decipher diffraction patterns, the JSPDS PDF 2 1911 database was used. Raman studies were carried out using excitation radiation with a wavelength of $\lambda_{ext} = 633$ nm.

The study of spectral and luminescent properties was carried out by optical spectroscopy using Eu^{3+} ions as a spectroscopic probe. Registration of luminescence spectra at $T = 300$ °K was carried out using an inVia spectrometer manufactured by RENISHAW.

The study of the transport characteristics of single-crystal and ceramic samples was carried out by impedance spectroscopy using a Solartron SI 1260 frequency response analyzer in the frequency range of 1–5 MHz with an alternating current signal amplitude of 24 mV in a temperature range of 350–900 °C with a step of 50° while holding at each temperature for 30–40 min. The samples were plates measuring 7×7 mm^2 with a thickness of 0.50 mm for single-crystal and 0.14 mm for ceramic samples. Impedance measurements were carried out using the four-contact method on samples with symmetrically located platinum electrodes. The electrodes were made of Pt paste, which was applied to the samples and then fired at a temperature of 950 °C for 1 h in air. Impedance spectra were processed using the ZView program (ver. 2.8). The electrical conductivity was calculated from data obtained by processing impedance spectra, taking into account the geometric dimensions of the samples.

Results and discussion

Figure 1 shows a diagram of the ceramic manufacturing process.

The results of X-ray diffraction analysis of the studied ceramic and single crystal samples $(ZrO_2)_{0.90}(Sc_2O_3)_{0.09}(Yb_2O_3)_{0.01}$ are shown in Fig. 2. The crystals were single-phase and had a cubic fluorite-type structure. Phase analysis of single crystals was carried out on plates cut from the central part of the crystals perpendicular to the <100> direction. As follows from Fig. 2, the grinding of single crystals and further operations for the production of ceramic samples did not lead to a change in the phase composition of the samples. The crystal lattice parameters also did not change and amounted to 0.5094 nm. The results of X-ray diffraction analysis of the studied ceramic samples indicate that they are single-phase and have a cubic fluorite-type structure.

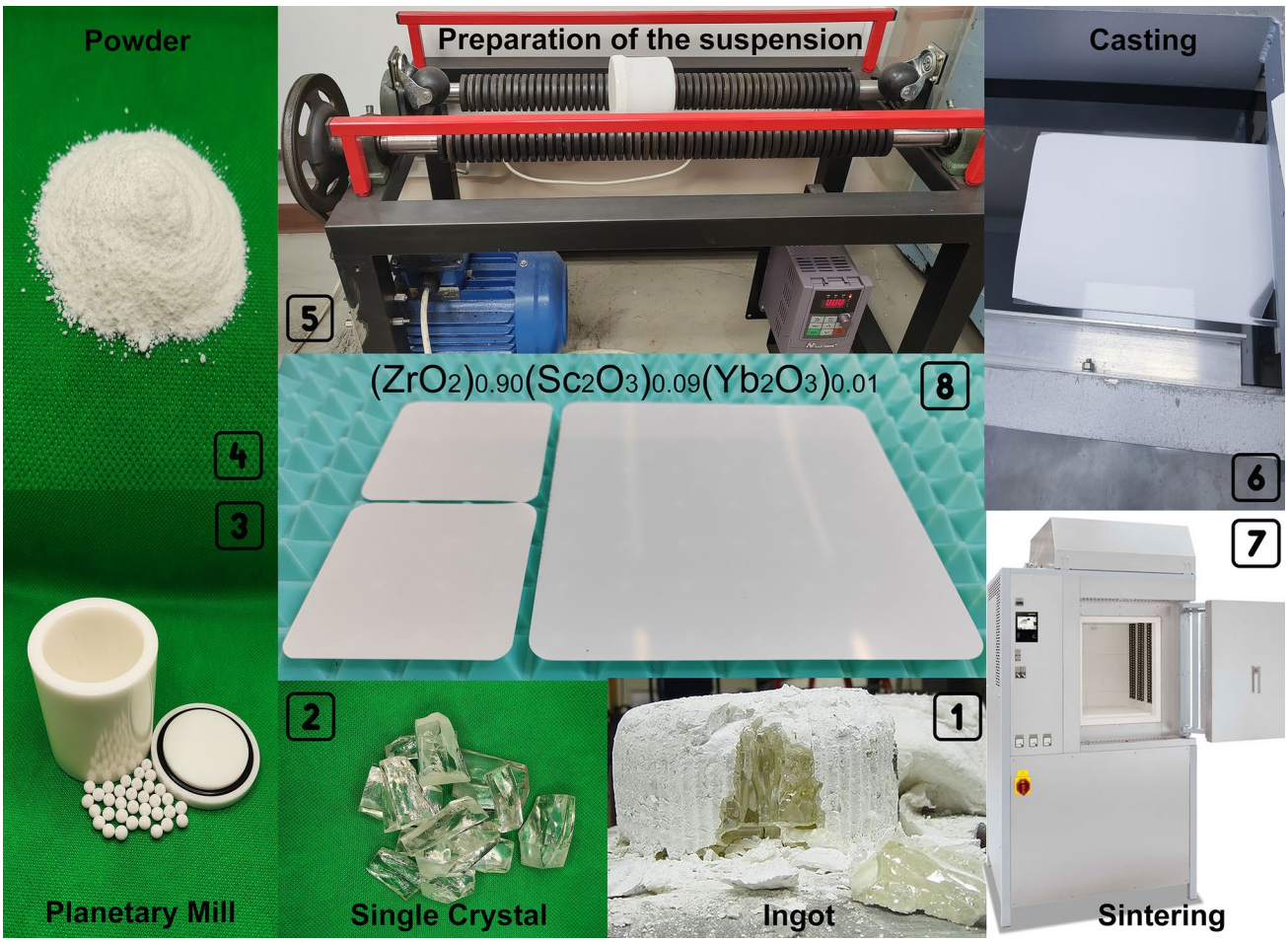

Fig. 1 Scheme of the ceramic manufacturing process

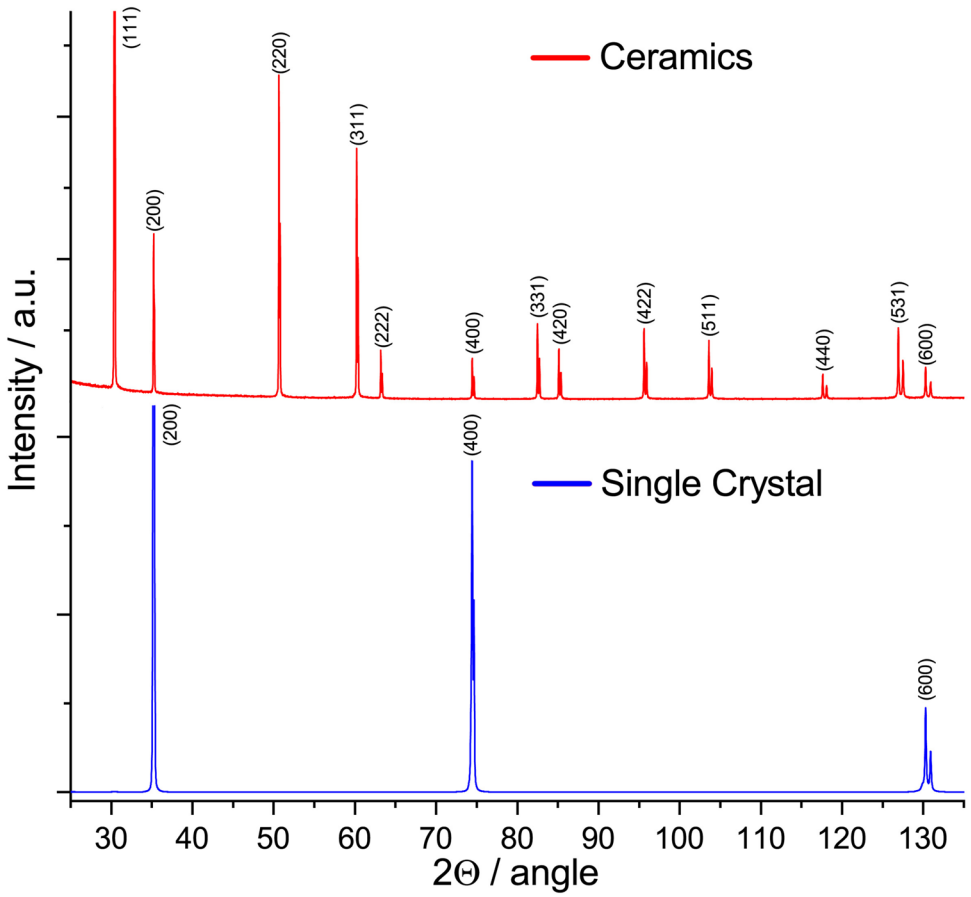

Fig. 2 X-ray diffraction patterns of the single crystal and ceramic sample $(ZrO_2)_{0.90}(Sc_2O_3)_{0.09}(Yb_2O_3)_{0.01}$

The structure and phase composition of the ceramics and the initial crystal were controlled by the Raman method. The Raman spectra of ceramics and single crystal $(ZrO_2)_{0.90}(Sc_2O_3)_{0.09}(Yb_2O_3)_{0.01}$ is shown in Fig. 3.

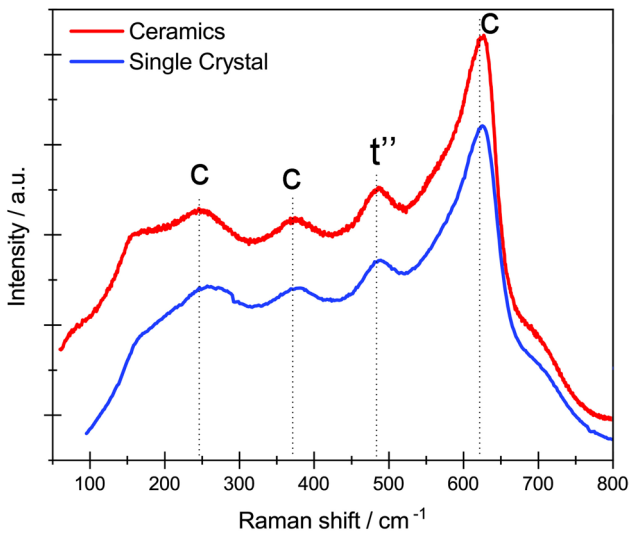

Fig. 3 Raman spectra of $(ZrO_2)_{0.90}(Sc_2O_3)_{0.09}(Yb_2O_3)_{0.01}$ ceramics and single crystal

The Raman spectra of the ceramics and single crystal indicated no detectable change in the chemical structure, formation of new peaks, or significant displacement of existing peak centers. In the given spectra of ceramics and crystals, peaks at 250 cm^{-1}, 365 cm^{-1}, and 610 cm^{-1} are observed, which belong to the cubic phase of zirconium dioxide. In addition, the spectra have a peak with a maximum of ~ 480 cm^{-1}, which is characteristic of the t″-phase structure close to cubic [32]. The coincidence of the patterns of the Raman spectra of ceramics at different points indicates that the phase composition is the same throughout the sample.

Figure 4 shows the microstructure of cross-section (a) and the surface (b) of the ceramic sample obtained using a scanning electron microscope.

The presence of isolated pores in the cross-section of the sample with dimensions of no more than 2–5 μm is visible. An analysis was carried out on the distribution of grain sizes (Fig. 5). The analysis showed that the ceramic grain size is in the range of ~ 1 to 10 μm. Most of the grains, ~ 50%, have sizes of up to ~ 5–6 μm.

Spectral analysis on a scanning electron microscope using the energy dispersive method did not show the presence of any foreign impurities.

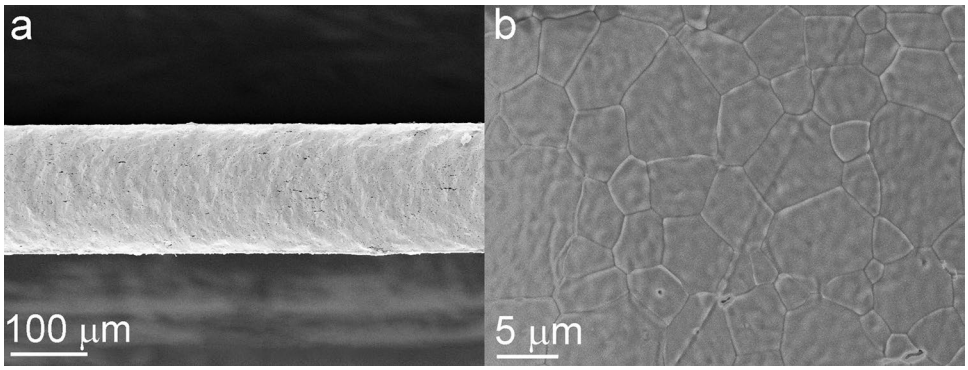

Fig. 4 SEM image of the cross section (**a**) and surface (**b**) of the ceramic sample

In this work, we used the excitation of Eu^{3+} ions to the $^5D_1$ level. Luminescence spectra were recorded for the transitions $^5D_0 \rightarrow {}^7F_0$, $^5D_0 \rightarrow {}^7F_1$, $^5D_0 \rightarrow {}^7F_2$, $^5D_0 \rightarrow {}^7F_3$, $^5D_0 \rightarrow {}^7F_4$.

Figure 6 shows the luminescence spectra of $(ZrO_2)_{0.90}(Sc_2O_3)_{0.09}(Yb_2O_3)_{0.01}$ single crystals and ceramics, recorded upon excitation by radiation with a wavelength of 532 nm at room temperature.

Analysis of the luminescence spectra for transitions between the $^5D_0$ and $^7F_{J(0-4)}$ multiplets of Eu^{3+} ions in $(ZrO_2)_{0.90}(Sc_2O_3)_{0.09}(Yb_2O_3)_{0.01}$ ceramics, recorded upon excitation of the $^5D_1$ level of Eu^{3+} ions at $T = 300$ °K indicates that they are characterized by the presence of the same spectral lines as for a similar spectrum of a single crystal. This indicates the same local oxygen environment of Eu^{3+} ions in single crystals and ceramics. During the process of grinding crystals and manufacturing ceramic samples, the material may become contaminated with uncontrolled impurities. Thus, in ceramic samples of zirconium dioxide stabilized with scandium oxide, also made from grounded crystals, the presence of intense additional lines associated with $Al_2O_3:Cr^{3+}$ impurity was noted in the luminescence spectrum [33]. No additional lines were detected in the luminescence spectra of $(ZrO_2)_{0.90}(Sc_2O_3)_{0.09}(Yb_2O_3)_{0.01}$ ceramics, which indicates the absence of external impurities in it.

Thus, the structural studies of ceramic samples made from grounded crystals using the tape-casting method showed that the phase composition, crystalline and local structure, as well as the crystal lattice parameter of the ceramics do not undergo changes compared to single crystals.

Figure 7 shows the characteristic impedance spectra of ceramic and single-crystal samples at various temperatures.

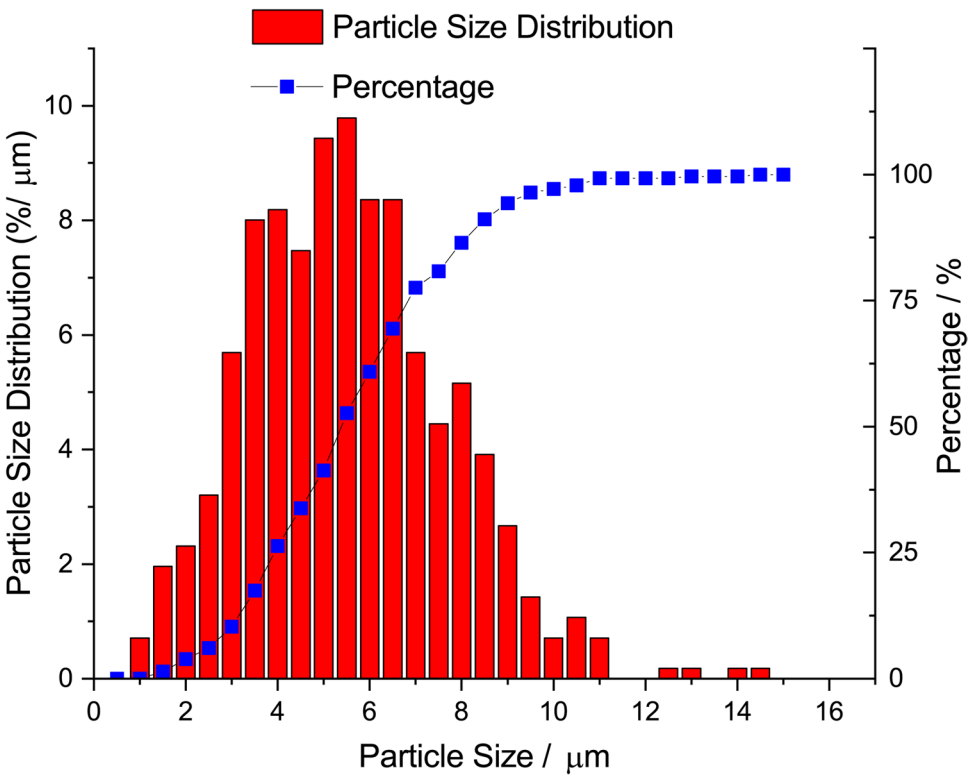

Fig. 5 Grain size distribution of $(ZrO_2)_{0.90}(Sc_2O_3)_{0.09}(Yb_2O_3)_{0.01}$ ceramic sample

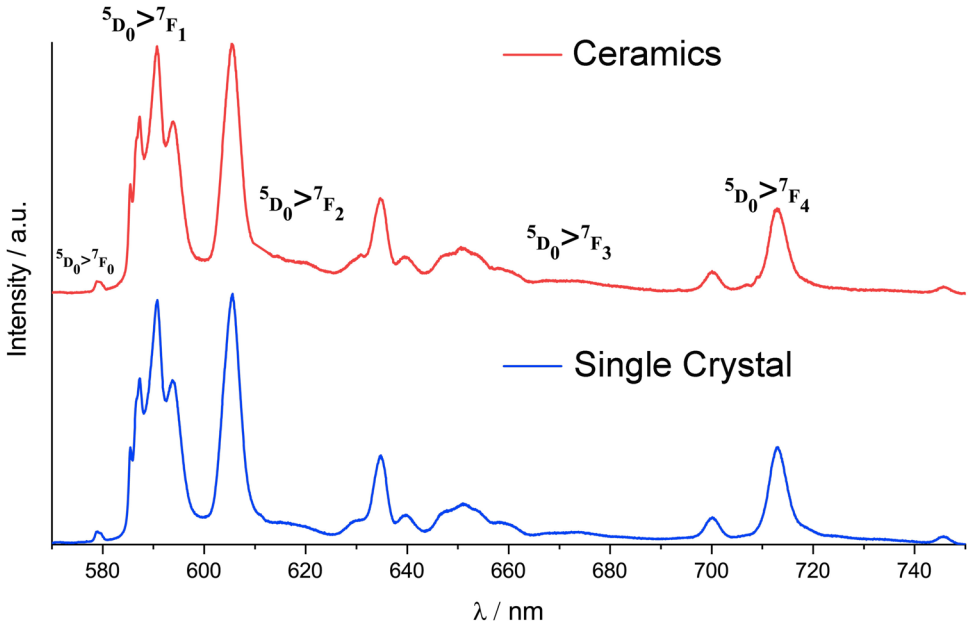

Fig. 6 Luminescence spectra of $(ZrO_2)_{0.90}(Sc_2O_3)_{0.09}(Yb_2O_3)_{0.01}$ single crystals and ceramics, $\lambda_{exc} = 532$ nm, $T = 300$ °K

When analyzing the impedance spectra of samples in the low-temperature region, the polarization contributions that relate to the material under study and the electrode/electrolyte interface are well-separated. For ceramic samples, an additional arc was observed in the impedance spectra in the high-frequency region, which is due to the contribution of the capacitive-resistive polarization of the electrolyte due to the partial blocking of oxygen ions at the grain boundaries of the electrolyte. For single-crystal samples, there is no additional arc in the impedance spectra due to the absence of grain boundaries. The volume resistance value of single crystals (R_b) was calculated within the framework of an equivalent electrical circuit model $(R_b - CPE_b)(R_{electrode} - CPE_{electrode})$ at low temperatures of 350–400 °C, and for ceramics, the volume resistance value was calculated within the framework of an equivalent electrical circuit model $(R_b - CPE_b)(R_{gb} - CPE_{gb})(R_{electrode} - CPE_{electrode})$. For the high-temperature range 450–900 °C, the equivalent circuit $LR_b(R_{electrode} - CPE_{electrode})$ for single crystals and ceramics was used, where $R_{electrode}$ is the resistance of the electrode/electrolyte interface, $CPE_{electrode}$ is a constant phase element characterizing processes at the electrode interface, R_{gb} is the resistance of the boundaries grains, CPE_{gb} is a constant phase element characterizing processes at grain boundaries, and L is the inductance of current leads.

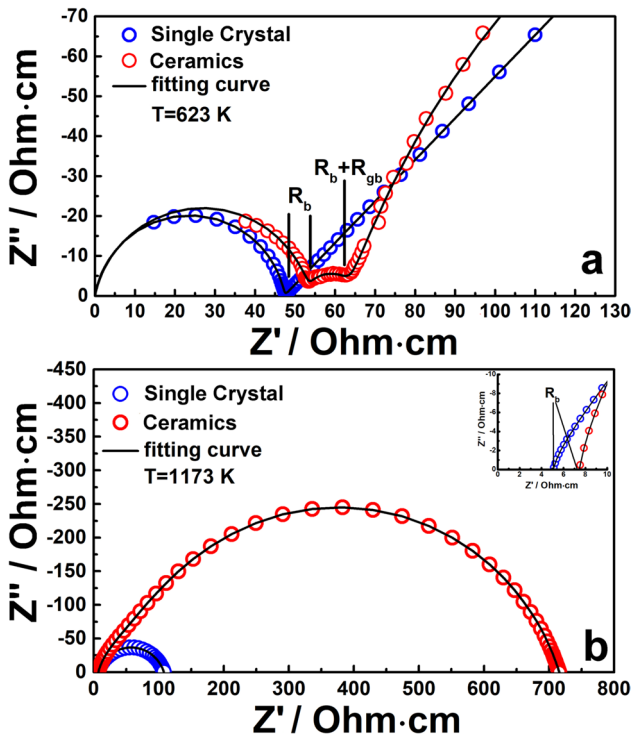

Fig. 7 Impedance spectra of $(ZrO_2)_{0.90}(Sc_2O_3)_{0.09}(Yb_2O_3)_{0.01}$ ceramics and single crystal at 623 (**a**) and 1173 °K (**b**)

Figure 8 shows the temperature dependencies of the electrical conductivity of single crystal and ceramic samples in Arrhenius coordinates. It was found that throughout the entire temperature range for ceramic and single-crystal solid electrolytes, the values of the electrical conductivity are different. A possible reason for this difference is the errors that arise in determining the geometric factor due to the presence of closed pores in the sample, as shown in the image of a cross-section of the ceramic sample. A decrease in the electrical conductivity of ceramics compared to a single crystal (from 0.176 to 0.235 S/cm, respectively, at 1173 °K) may also be associated with an increased electrical resistance of grain boundaries. The non-uniform distribution of oxygen

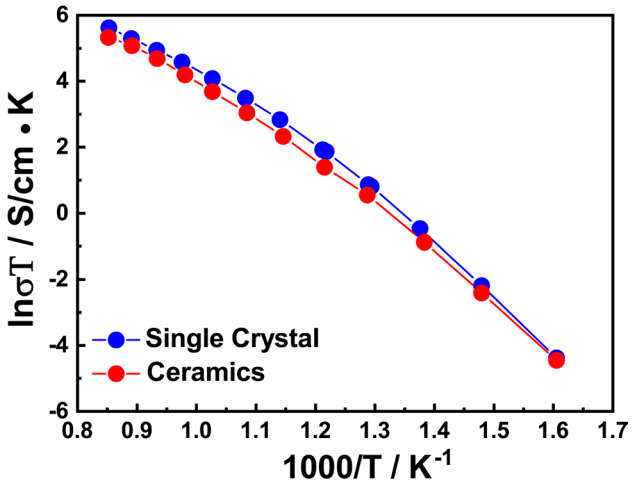

Fig. 8 Temperature dependences of the electrical conductivity of single crystal and ceramic samples

vacancies at grain boundaries leads to the appearance of a space charge at these boundaries and to an increase in electrical resistance even in high-purity ceramics [34].

From Fig. 8, it is clearly seen that the temperature dependences of the electrical conductivity of single crystal and ceramic samples in Arrhenius coordinates are nonlinear, which indicates a different conductivity mechanism in different temperature ranges.

Activation energy for electrical conductivity (E_a) was calculated from impedance data in two temperature ranges of 350–500 and 750–900 °C. The E_a values of the single crystal and ceramic sample in the low-temperature region were 1.43 ± 0.02 and 1.36 ± 0.02 eV, respectively; in the high-temperature region, these values were 0.73 ± 0.03 and 0.76 ± 0.03 eV. In accordance with the model proposed in [35], in oxygen-ion conductors, such as solid solutions based on zirconium dioxide, E_a in the low-temperature region consists of the migration energy of oxygen vacancies (E_m) and the association energy (E_{as}). E_{as} is the energy required to dissociate different types of clusters containing vacancies. At high temperatures, free migration of isolated vacancies occurs, and E_a is equal to the enthalpy of migration. The data obtained show that E_m in single-crystal and ceramic samples does not differ within the measurement error.

Thus, the electrical conductivity of the ceramic samples is close to the electrical conductivity of single crystals. A slight decrease in conductivity is associated with the characteristics of the ceramic microstructure, namely the presence of residual porosity, grain size, and the presence of grain boundaries. These characteristics are determined by the conditions of the sintering of ceramic samples. It is obvious that changes in sintering conditions aimed at increasing the density of ceramics can bring its conductivity closer to the conductivity values of a single-crystal material.

Conclusions

Ceramic solid electrolytes $(ZrO_2)_{0.90}(Sc_2O_3)_{0.09}(Yb_2O_3)_{0.01}$ were obtained from powders prepared by grinding single crystals of the same chemical composition. The grain size of ceramics is in the range from ~ 1 to 10 μm. The maximum particle size distribution was at ~ 5 μm. In the cross-section of the samples, there were a small number of closed pores with sizes up to ~ 2–5 μm.

A comparative analysis of the structure of ceramic and single crystal samples showed that the phase composition, crystalline and local structure, as well as the crystal lattice parameter of ceramics do not undergo changes compared to single crystals. Both of these samples had the structure of a pseudocubic t″-phase. The electrical conductivity of ceramics was less than the electrical conductivity of a single crystal over the entire temperature range. The observed differences in electrical conductivity are likely due to the presence of pores and grain boundaries in ceramic samples.

Funding This work was financially supported by the Moscow Polytechnic University within the framework of the grant named after Pyotr Kapitsa.

References

1. Goodenough JB (2003) Oxide-ion electrolytes Annu Rev Mater Res 33:91
2. Kharton VV, Marques FMB, Atkinson A (2004) Transport properties of solid oxide electrolyte ceramics: a brief review. Solid State Ion 174:135
3. Vinchhi P, Khandl M, Chaudhary K, Pati R (2023) Recent advances on electrolyte materials for SOFC: a review. Inorg Chem Comm 152:110724
4. Hussain S, Yangping L (2020) Review of solid oxide fuel cell materials: cathode, anode, and electrolyte. Energ Trans 4:113–126
5. Yamamoto O (2000) Solid oxide fuel cells: fundamental aspects and prospects. Electrochim Acta 45(15–16):2423
6. Wachsman ED, Lee KT (2011) Lowering the temperature of solid oxide fuel cells. Science 334:935
7. Han F, Mücke R, Gestel TV, Leonide A, Menzler NH, Buchkremer HP, Stöver D (2012) Novel high-performance solid oxide fuel cells with bulk ionic conductance dominated thin-film electrolytes. J Power Sources 218:157
8. Zhigachev AO, Rodaev VV, Zhigacheva DV, Lyskov NV, Shchukina MA (2021) Doping of scandia-stabilized zirconia electrolytes for intermediate-temperature solid oxide fuel cell: a review. Ceram Int 47:32490–32504
9. Mojaver P, Chitsaz A, Sadeghi M, Khalilarya S (2020) Comprehensive comparison of SOFCs with proton-conducting electrolyte and oxygen ion-conducting electrolyte: thermoeconomic analysis and multiobjective optimization. Energ Conv Manag 205:112455
10. Khajavi P, Hendriksen PV, Chevalier J, Gremillard L, Frandsen HL (2020) Improving the fracture toughness of stabilized zirconia-based solid oxide cells fuel electrode supports: effects of type and concentration of stabilizer(s). J Europ Ceram Soc 40:5670–5682

11. Omar S, Belda A, Escardino A, Bonanos N (2010) Ionic conductivity ageing investigation of 1Ce10ScSZ in different partial pressures of oxygen. Solid State Ion 184:2
12. Jais AA, Ali SAM, Anwar M, Somalu MR, Muchtar A, Isahak WNRW, Tan CY, Singh R, Brandon NP (2017) Enhanced ionic conductivity of scandia-ceria-stabilized-zirconia (10Sc1CeSZ) electrolyte synthesized by the microwave-assisted glycine nitrate process. Ceram Int 43(11):8119
13. Kumar A, Jaiswa A, Sanbui M, Omar S (2016) Oxygen-ion conduction in scandia-stabilized zirconia-ceria solid electrolyte (xSc2O3 − 1CeO2 − (99–x)ZrO2, 5 ≤ x ≤ 11). J Am Ceram Soc 100:659–668
14. Lee D-S, Kim WS, Choi SH, Kim J, Lee H-W, Lee J-H (2005) Characterization of ZrO_2 co-doped with Sc_2O_3 and CeO_2 electrolyte for the application of intermediate temperature SOFCs. Solid State Ion 176(1–2):33
15. Abbas HA, Argirusis C, Kilo M, Wiemhöfer H-D, Hammad FF, Hanafi ZM (2011) Preparation and conductivity of ternary scandia-stabilised zirconia. Solid State Ion 184(1):6
16. Spirin A, Ivanov V, Nikonov A, Lipilin A, Paranin S, Khrustov V, Spirina A (2012) Scandia-stabilized zirconia doped with yttria: synthesis, properties, and ageing behavior. Solid State Ion 225:448
17. Omar S, Najib WB, Chen W (1965) Bonanos N (2012) Electrical conductivity of 10 mol% Sc_2O_3–1 mol% M_2O_3–ZrO_2 ceramics. J Am Ceram Soc 95:6
18. Araki W, Koshikawa T, Yamaji A, Adachi T (2009) Degradation mechanism of scandia-stabilised zirconia electrolytes: discussion based on annealing effects on mechanical strength, ionic conductivity, and Raman spectrum. Solid State Ion 180(28–31):1484
19. Hirano M, Watanabe S, Kato E, Mizutani Y, Kawai M, Nakamura Y (1999) High electrical conductivity and high fracture strength of Sc_2O_3-doped zirconia ceramics with submicrometer grains. J Am Ceram Soc 82(10):2861
20. Hui SR, Roller J, Yick S, Zhang X, Decés-Petit C, Xie Y, Maric R, Ghosh D (2007) A brief review of the ionic conductivity enhancement for selected oxide electrolytes. J Power Sources 172(2):493
21. Mathur L, Namgung Y, Kim K, Song S-J (2023) Recent progress in electrolyte-supported solid oxide fuel cells: a review. J Korean Ceram Soc 60:614–636
22. Osiko VV, Borik MA, Lomonova EE (2010) Handbook of crystal growth. Springer, Berlin, pp 433–469
23. Borik MA, Bredikhin SI, Bublik VT, Kulebyakin AV, Kuritsyna IE, Lomonova EE, Milovich FO, Myzina VA, Osiko VV, Ryabochkina PA, Tabachkova NYu (2017) Structure and conductivity of yttria and scandia-doped zirconia crystals grown by skull melting. J Am Ceram Soc 100(12):5536–5547
24. Agarkov DA, Borik MA, Bublik VT, Bredikhin SI, Chislov AS, Kulebyakin AV, Kuritsyna IE, Lomonova EE, Milovich FO, Myzina VA, Osiko VV, Tabachkova NYu (2018) Structure and transport properties of melt grown Sc2O3 and CeO2 doped ZrO2 crystals. Solid State Ion 322:24–29
25. Agarkov DA, Borik MA, Bredikhin SI, Burmistrov IN, Eliseeva GM, Kolotygin VA, Kulebyakin AV, Kuritsyna IE, Lomonova EE, Milovich FO, Myzina VA, Ryabochkina PA, Tabachkova NYu, Volkova TV (2019) Structure and transport properties of zirconia crystals co-doped by scandia, ceria and yttria. J Mater 5:273–279
26. Agarkov DA, Borik MA, Bredikhin SI, Burmistrov IN, Eliseeva GM, Kulebyakin AV, Kuritsyna IE, Lomonova EE, Milovich FO, Myzina VA, Tabachkova NYu (2020) Phase compositions, structures and properties of scandia-stabilized zirconia solid solution crystals co-doped with yttria or ytterbia and grown by directional melt crystallization. Solid State Ion 346:115218
27. Kulebyakin AV, Borik MA, Kuritsyna IE, Larina NA, Lomonova EE, Milovich FO, Myzina VA, Ryabochkina PA, Skryleva EA, Tabachkova NYu, Volkova TV (2020) Structural characteristics of melt-grown $(ZrO_2)_{0.99-x}(Sc_2O_3)_x(Yb_2O_3)_{0.01}$ solid solution crystals and their effect on ionic conductivity. J Crystal Growth 547:125808. https://doi.org/10.1016/j.jcrysgro.2020.125808, https://www.sciencedirect.com/science/article/pii/S0022024820303316
28. Agarkov D, Borik M, Komarov B, Korableva G, Kulebyakin A, Kuritsyna I, Lomonova E, Milovich F, Myzina V, Tabachkova N (2023) Long-term conductivity stability of electrolytic membranes of scandia stabilized zirconia co-doped with ytterbia. Membranes 13:586
29. Shukla V, Balani K, Subramaniam A, Omar S (2019) Effect of thermal aging on the phase stability of 1Yb2O3−xSc2O3−(99–x) ZrO2 (x = 7, 8 mol %.). J Phys Chem C 123:21982–21992
30. Lakshmi VV, Bauri R (2011) Phase formation and ionic conductivity studies on ytterbia co-doped scandia stabilized zirconia (0.9ZrO2–0.9Sc2O3–0.01Yb2O3) electrolyte for SOFCs. Solid State Sci 13(8):1520–1525
31. Yamaji A, Koshikawa T, Araki W, Adachi T (2008) Stabilization of a zirconia system and evaluation of its electrolyte characteristics for a fuel cell: based on electrical and mechanical considerations. J Eng Mater Technol 131(1):011010
32. Hemberger Y, Wichtner N, Berthold C, Nickel KG (2016) Quantification of yttria in stabilized zirconia by Raman spectroscopy. Int J Appl Ceram Technol 13:116–124
33. Agarkov D, Borik M, Buzaeva E, Korableva G, Kulebyakin A, Kuritsyna I, Larina N, Kyashkin V, Lomonova E, Milovich F, Myzina V, Ryabochkina P, Tabachkova N, Zakharov D (2023) Structure and physical properties of ceramic materials based on ZrO2-Sc2O3 for SOFC electrolytic membranes obtained from powders of melted solid solutions with a similar composition. Membranes 13:717
34. Guo X, Maier J (2001) Grain boundary blocking effect in zirconia: a Schottky barrier analysis. J Electrochem Soc 148(3):E121
35. Kilner JA, Steele BCH (1981) In: Sorensen OT (ed) Non-stoichiometric oxides. Academic Press, New York, pp 233–269. https://books.google.ru/books?hl=ru&lr=&id=bUMsPXFE8ToC&oi=fnd&pg=PP1&ots=qjBeCex9nY&sig=FtJHO4evBi2E0O-ZctIwSrVg7Sc&redir_esc=y#v=onepage&q&f=false